Impact Factor:					
	ISRA (India)	= 6.317	SIS (USA)	= 0.912	ICV (Poland)	= 6.630
	ISI (Dubai, UAE)	= 1.582	РИНЦ (Russia)	= 3.939	PIF (India)	= 1.940
	GIF (Australia)	= 0.564	ESJI (KZ)	= 9.035	IBI (India)	= 4.260
	JIF	= 1.500	SJIF (Morocco)	= 7.184	OAJI (USA)	= 0.350

SOI: 1.1/TAS DOI: 10.15863/TAS

International Scientific Journal

Theoretical & Applied Science

p-ISSN: 2308-4944 (print) **e-ISSN:** 2409-0085 (online)

Year: 2021 **Issue:** 12 **Volume:** 104

Published: 29.12.2021 **http://T-Science.org**

QR – Issue QR – Article

Denis Chemezov
Vladimir Industrial College
M.Sc.Eng., Corresponding Member of International Academy of Theoretical and Applied Sciences, Lecturer, Russian Federation
https://orcid.org/0000-0002-2747-552X
vic-science@yandex.ru

Vladislav Gonchar
Vladimir Industrial College
Student, Russian Federation

Artyom Gamanistov
Vladimir Industrial College
Student, Russian Federation

Dmitriy Satarin
Vladimir Industrial College
Student, Russian Federation

Talabsho Kamilov
Vladimir Industrial College
Student, Russian Federation

Nikolay Kornev
Vladimir Industrial College
Student, Russian Federation

Egor Tuykin
Vladimir Industrial College
Student, Russian Federation

REFERENCE DATA OF PRESSURE DISTRIBUTION ON THE SURFACES OF AIRFOILS HAVING THE NAMES BEGINNING WITH THE LETTER D

Abstract: *The results of the computer calculation of air flow around the airfoils having the names beginning with the letter D are presented in the article. The contours of pressure distribution on the surfaces of the airfoils at the angles of attack of 0, 15 and -15 degrees in conditions of the subsonic airplane flight speed were obtained.*

Key words: *the airfoil, the angle of attack, pressure, the surface.*

Language: *English*

Citation: Chemezov, D., et al. (2021). Reference data of pressure distribution on the surfaces of airfoils having the names beginning with the letter D. *ISJ Theoretical & Applied Science, 12 (104)*, 1244-1274.

Soi: http://s-o-i.org/1.1/TAS-12-104-140 ***Doi***: https://dx.doi.org/10.15863/TAS.2021.12.104.140

Scopus ASCC: *1507.*

Introduction

Creating reference materials that determine the most accurate pressure distribution on the airfoils surfaces is an actual task of the airplane aerodynamics.

Materials and methods

The study of air flow around the airfoils was carried out in a two-dimensional formulation by means of the computer calculation in the *Comsol Multiphysics* program. The airfoils in the cross section were taken as objects of research [1-14]. In this work, the airfoils having the names beginning with the letter *D* were adopted. Air flow around the airfoils was carried out at the angles of attack (α) of 0, 15 and -15 degrees. The flight speed of the airplane in each case was subsonic. The airplane flight in the atmosphere was carried out under normal weather conditions. The geometric characteristics of the studied airfoils are presented in the Table 1. The geometric shapes of the airfoils in the cross section are presented in the Table 2.

Table 1. The geometric characteristics of the airfoils.

Airfoil name	Max. thickness	Max. camber	Leading edge radius	Trailing edge thickness
D6	7.4% at 20.0% of the chord	6.9% at 30.0% of the chord	0.9317%	0.2%
DA0101	5.3% at 30.0% of the chord	6.3% at 40.0% of the chord	1.2254%	0.0%
DA093017	9.2% at 30.0% of the chord	5.85% at 40.0% of the chord	0.8866%	0.0%
DA1002	10.5% at 30.0% of the chord	6.35% at 40.0% of the chord	1.0674%	0.0%
DA100B20	10.5% at 30.0% of the chord	6.35% at 40.0% of the chord	1.6056%	0.0%
DA93B17	9.2% at 30.0% of the chord	5.85% at 40.0% of the chord	0.8866%	0.0%
DAB76B17	9.17% at 30.0% of the chord	5.86% at 40.0% of the chord	0.8927%	0.0%
DAB80B20	10.46% at 30.0% of the chord	6.34% at 40.0% of the chord	1.0297%	0.0%
DAE-11	12.81% at 31.5% of the chord	6.62% at 44.4% of the chord	1.3641%	0.0%
DAE-21	11.78% at 31.8% of the chord	6.57% at 44.6% of the chord	1.8569%	0.0%
DAE-31	11.06% at 29.2% of the chord	6.75% at 45.1% of the chord	2.186%	0.0%
DAE-51	9.38% at 30.7% of the chord	4.02% at 43.3% of the chord	0.8406%	0.2%
DAN-MP	6.8% at 20.0% of the chord	7.25% at 40.0% of the chord	1.3239%	0.0%
David Fraser DF 101	10.99% at 29.8% of the chord	2.3% at 45.2% of the chord	0.874%	0.007%
David Fraser DF 102	10.99% at 29.8% of the chord	2.3% at 45.2% of the chord	0.9725%	0.007%
Davis	11.25% at 30.0% of the chord	3.69% at 40.0% of the chord	0.8876%	0.0%
DAVIS BASIC B-24 WING	15.89% at 27.9% of the chord	2.47% at 31.7% of the chord	1.9735%	0.0%
DAVIS-N	7.42% at 30.0% of the chord	5.85% at 50.0% of the chord	0.7303%	0.4%
davissm	5.87% at 30.6% of the chord	5.91% at 45.4% of the chord	0.6009%	1.178%
Dayton-Wright T-1	13.37% at 30.0% of the chord	7.06% at 40.0% of the chord	1.7369%	0.21%
dd928416	8.41% at 31.0% of the chord	1.55% at 36.0% of the chord	0.4303%	0.0%
DEFIANT CANARD BL110	14.73% at 28.6% of the chord	3.81% at 28.6% of the chord	1.0025%	0.0%
DEFIANT CANARD BL145	11.48% at 28.6% of the chord	2.38% at 28.6% of the chord	1.6191%	0.0%
DEFIANT CANARD BL20	20.92% at 28.6% of the chord	4.46% at 36.1% of the chord	3.0657%	0.0%
Delta 400	8.31% at 23.7% of the chord	1.6% at 27.9% of the chord	0.629%	0.0%
Delta 400 + 13%	9.39% at 23.7% of the chord	1.6% at 27.9% of the chord	0.7631%	0.0%
Delta 400 + 26%	10.47% at 23.7% of the chord	1.6% at 27.9% of the chord	0.9182%	0.0%
Delta 400 + 40%	11.64% at 23.7% of the chord	1.6% at 27.9% of the chord	1.1081%	0.0%
DF 101	10.99% at 29.8% of the chord	2.3% at 45.2% of the chord	0.874%	0.007%
DF102	10.99% at 29.8% of the chord	2.3% at 45.2% of the chord	0.9725%	0.007%
DFVLR R-4	13.38% at 38.1% of the chord	2.1% at 80.5% of the chord	1.205%	0.5099%
DFVLR R-4 transonic airfoil	13.38% at 38.1% of the chord	2.1% at 80.5% of the chord	1.2028%	0.51%
DFVLR RA 02	9.21% at 30.0% of the chord	3.16% at 40.0% of the chord	0.9713%	0.0%
DGA 1182	6.7% at 40.0% of the chord	1.0% at 30.0% of the chord	0.5247%	0.3%
dh4009sm	8.95% at 41.6% of the chord	0.2% at 9.6% of the chord	0.3752%	0.028%
Dicke 12,28%	12.25% at 32.4% of the chord	0.0% at 0.0% of the chord	0.7631%	0.0%
Dormoy	9.0% at 30.0% of the chord	4.54% at 20.0% of the chord	0.5718%	0.0%
DORNIER A-5	16.21% at 40.1% of the chord	2.54% at 78.0% of the chord	2.3431%	0.0%
DOUGLAS LA203A	15.73% at 34.3% of the chord	5.48% at 46.0% of the chord	3.0242%	0.0%
Douglas/Liebeck LA203A	15.73% at 34.3% of the chord	5.48% at 46.0% of the chord	3.0235%	0.0%
Douglas/Liebeck LNV109A	12.99% at 23.5% of the chord	5.97% at 31.5% of the chord	3.494%	0.0%
DRAGONFLY CANARD	19.34% at 37.4% of the chord	6.56% at 39.4% of the chord	1.399%	0.0%
Drela DAE11	12.81% at 31.5% of the chord	6.62% at 44.4% of the chord	1.3649%	0.0%
Drela DAE21	11.78% at 31.8% of the chord	6.57% at 44.6% of the chord	1.8593%	0.0%
Drela DAE31	11.06% at 29.2% of the chord	6.75% at 45.1% of the chord	2.1875%	0.0%
Drela DAE51	9.38% at 30.7% of the chord	4.02% at 43.3% of the chord	0.8408%	0.2%
DSMA-523A	11.0% at 36.0% of the chord	2.3% at 82.0% of the chord	2.4138%	-0.019%
DSMA-523B	11.0% at 36.0% of the chord	2.04% at 82.0% of the chord	2.4138%	1.0417%
DU 86-137-25	13.65% at 41.2% of the chord	0.28% at 1.4% of the chord	0.8062%	0.0%
DU86-084-18 8,44%	8.45% at 35.1% of the chord	1.12% at 44.4% of the chord	0.4786%	0.0%

DU868418	8.61% at 35.8% of the chord	1.14% at 45.2% of the chord	0.3825%	0.119%
Dunham	9.6% at 30.0% of the chord	1.0% at 30.0% of the chord	0.8799%	0.0%

Note:
David Fraser DF 101 (Low Reynolds number airfoil (Soartech 8));
David Fraser DF 102 (Low Reynolds number airfoil);
Dayton-Wright T-1 (W. Wright (USA));
DFVLR RA 02 (Germany);
DGA 1182 (Italy);
Dormoy (J. Dormoy (Great Britain));
Douglas/Liebeck LA203A, Douglas/Liebeck LNV109A (High lift airfoil);
Drela DAE11, Drela DAE21, Drela DAE31, Drela DAE51 (Low Reynolds number airfoil);
Dunham (B. Dunham (USA)).

Table 2. The geometric shapes of the airfoils in the cross section.

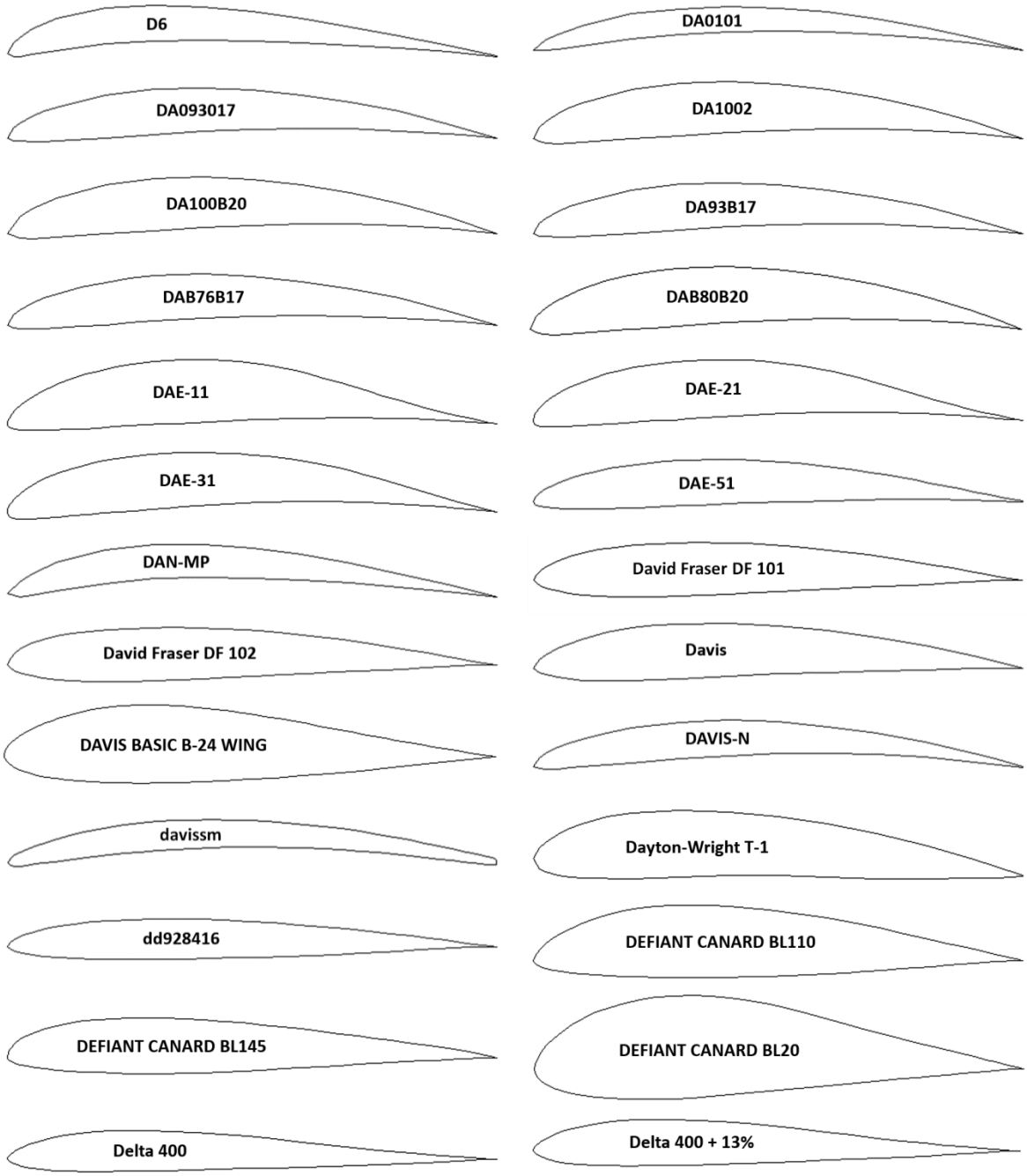

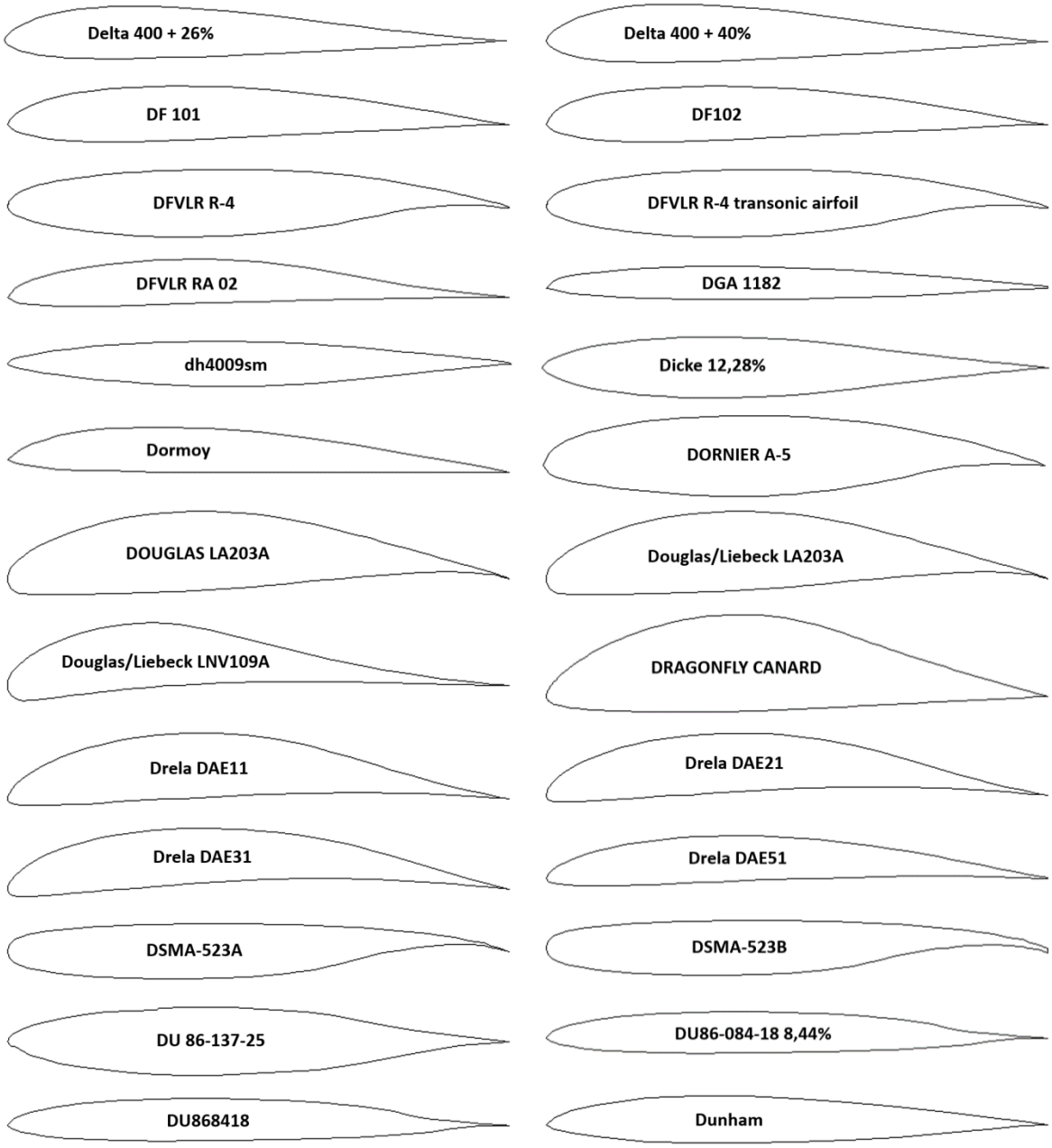

Results and discussion

The calculated pressure contours on the surfaces of the airfoils at the different angles of attack are presented in the Figs. 1-52.

The calculated magnitudes on the scale can be represented as the basic magnitudes when comparing the pressure drop under conditions of changing the angle of attack of the airfoils.

The presented range of the airfoils is characterized by curvature and asymmetry of the geometric shapes. There are modifications that differ by changing the size of the leading edge radius and the trailing edge thickness.

Air flows around the DF 101 airfoil in the horizontal position is accompanied by pressure of 7.22 kPa at the leading edge, which is the greatest pressure compared to the other airfoils experiencing loads under similar flight conditions. Thus, the drag on the leading edge of the DF 101 airfoil is 5-14% greater than that of the other airfoils.

The greatest difference of negative and positive pressures (18 times) between the upper and lower surfaces was determined for the DA0101 airfoil at the angle of attack of 15 degrees. This indicates the large lift of the airfoil. The smallest difference of negative and positive pressures (1.5 times) between the upper and lower surfaces was determined for the same airfoil at the angle of attack of -15 degrees.

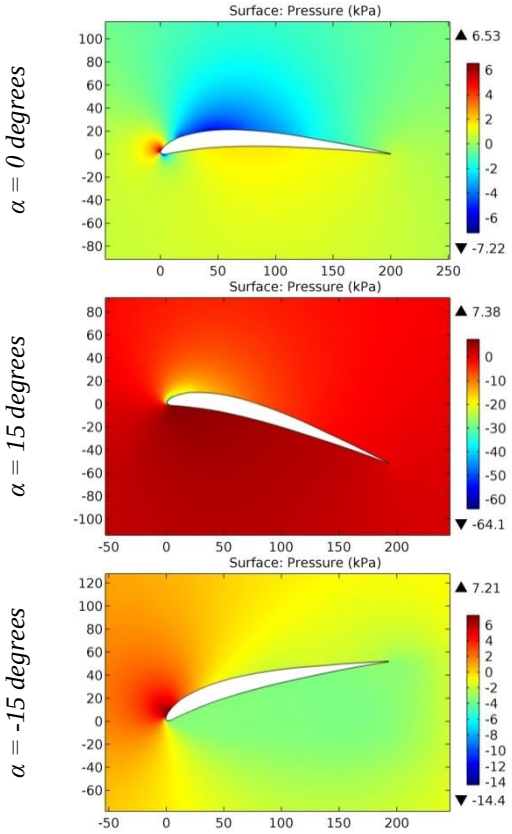

Figure 1. The pressure contours on the surfaces of the D6 airfoil.

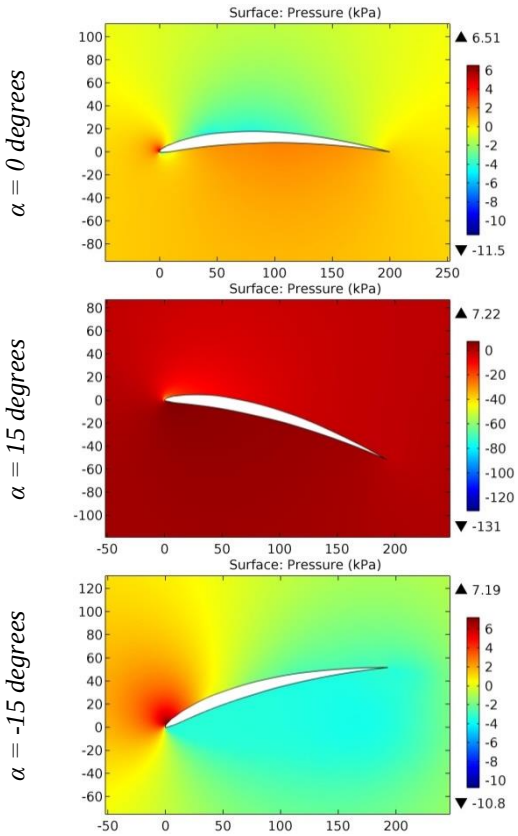

Figure 2. The pressure contours on the surfaces of the DA0101 airfoil.

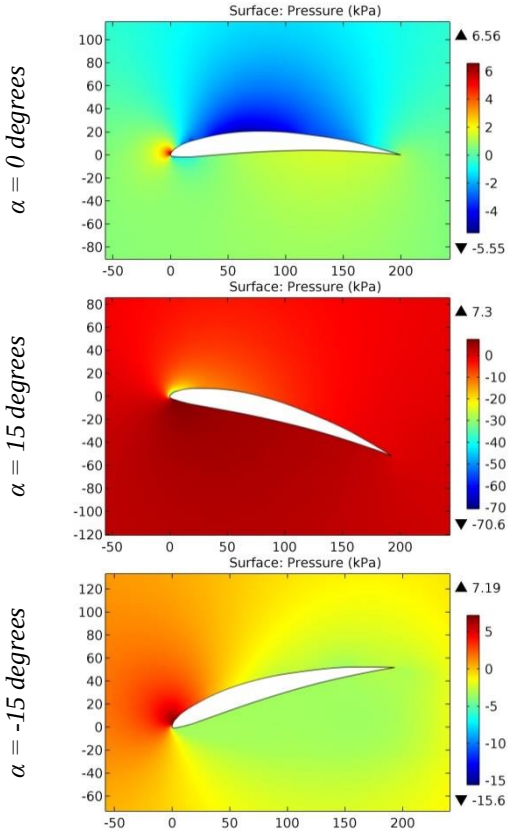

Figure 3. The pressure contours on the surfaces of the DA093017 airfoil.

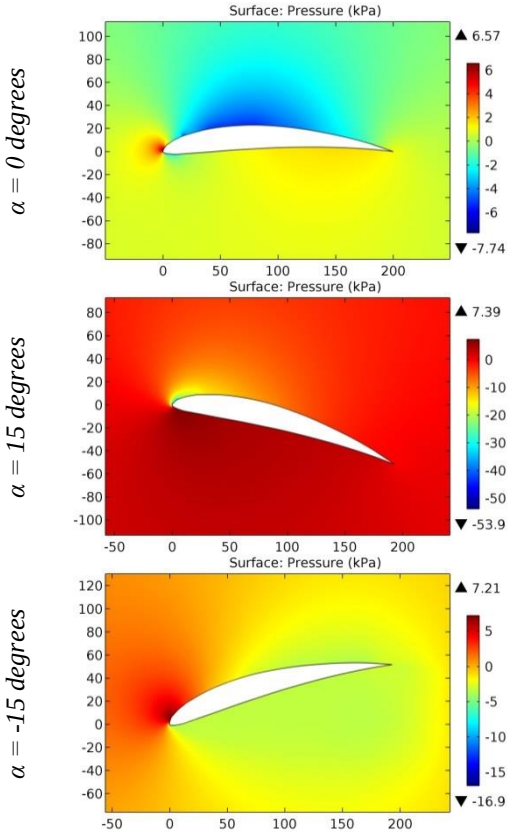

Figure 4. The pressure contours on the surfaces of the DA1002 airfoil.

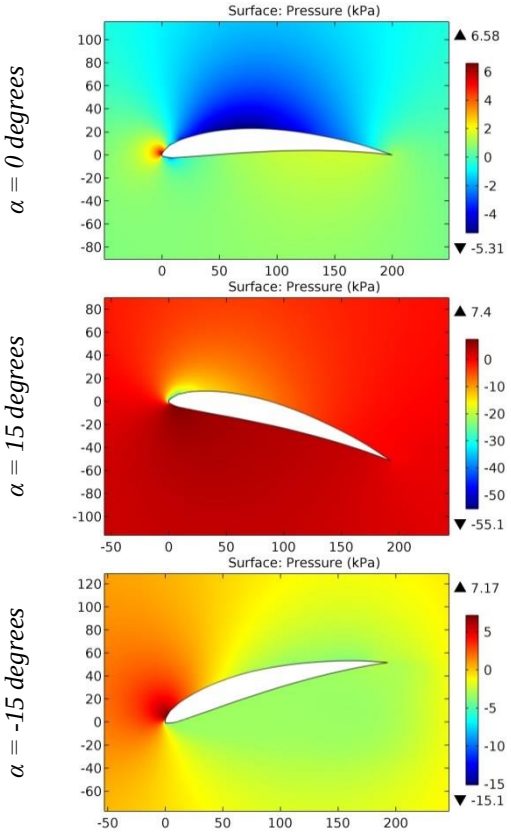

Figure 5. The pressure contours on the surfaces of the DA100B20 airfoil.

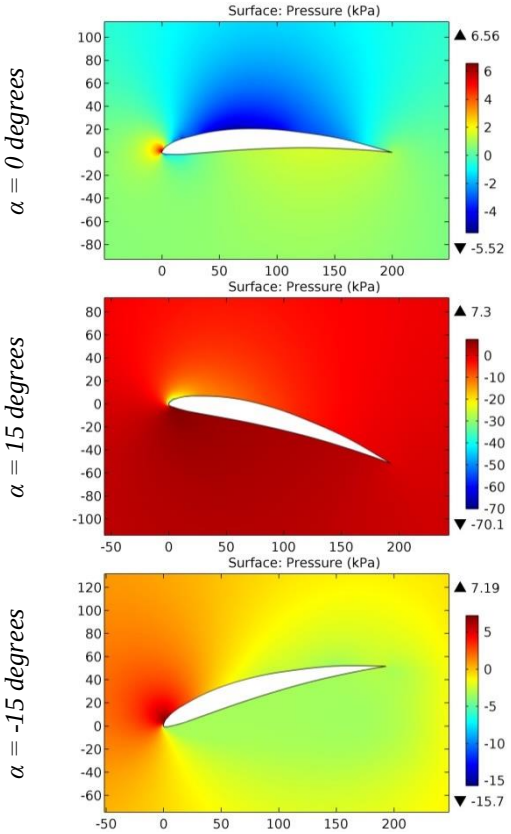

Figure 6. The pressure contours on the surfaces of the DA93B17 airfoil.

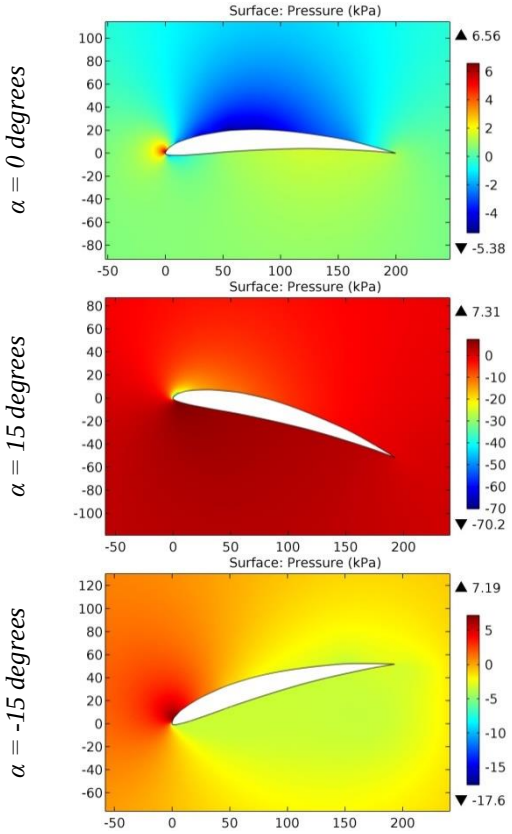

Figure 7. The pressure contours on the surfaces of the DAB76B17 airfoil.

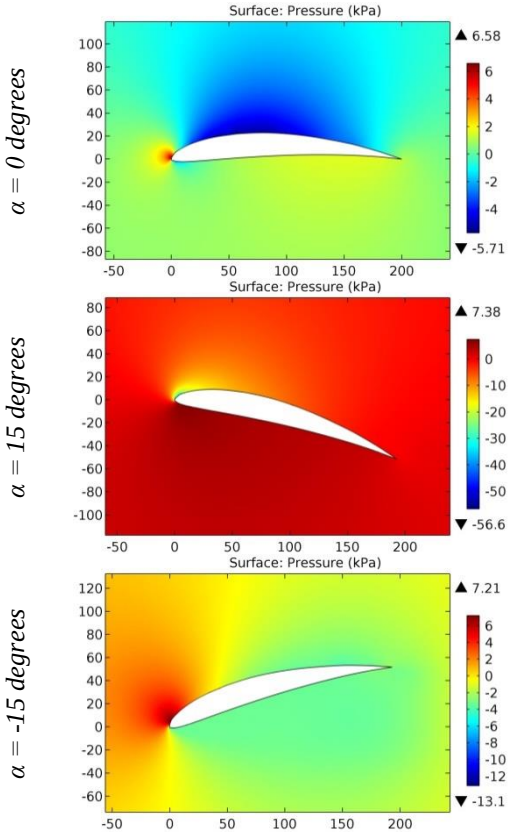

Figure 8. The pressure contours on the surfaces of the DAB80B20 airfoil.

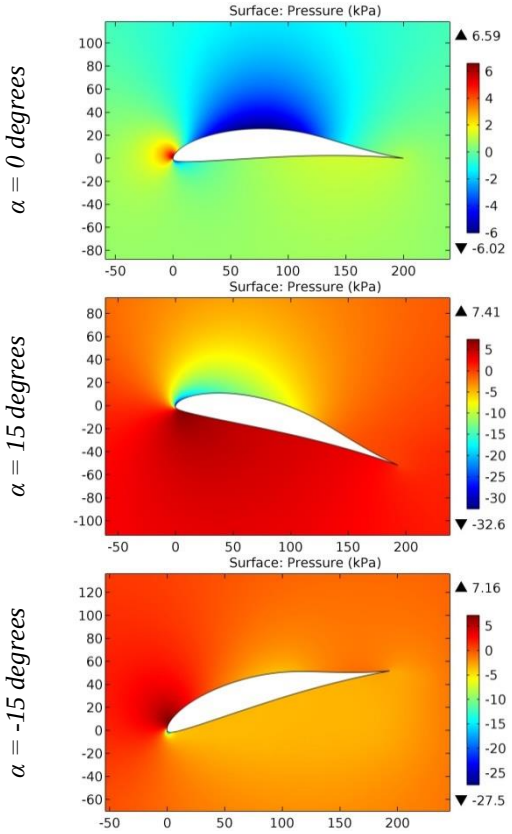

Figure 9. The pressure contours on the surfaces of the DAE-11 airfoil.

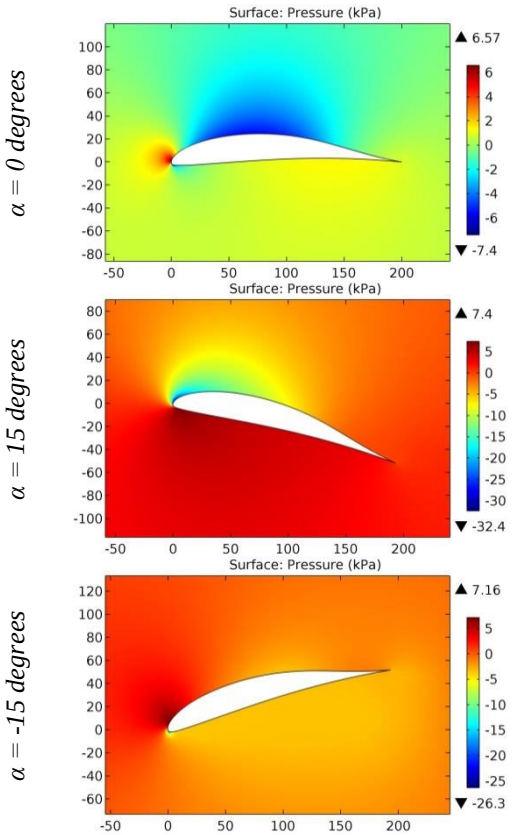

Figure 10. The pressure contours on the surfaces of the DAE-21 airfoil.

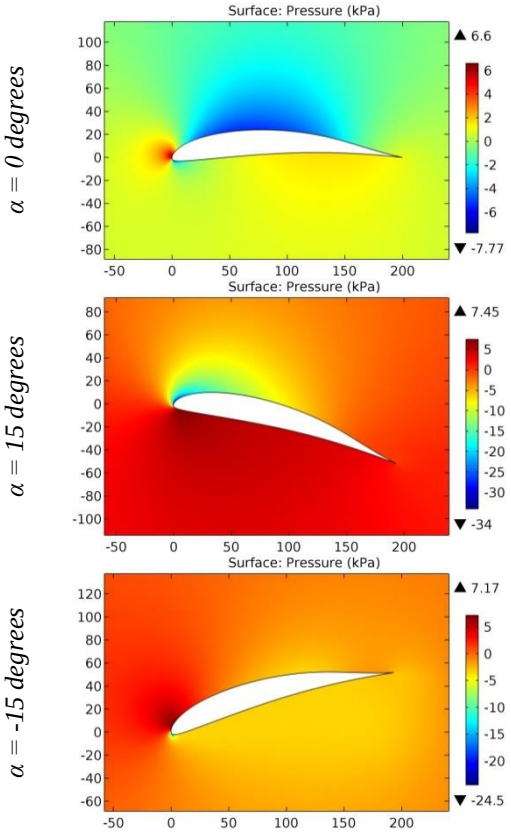

Figure 11. The pressure contours on the surfaces of the DAE-31 airfoil.

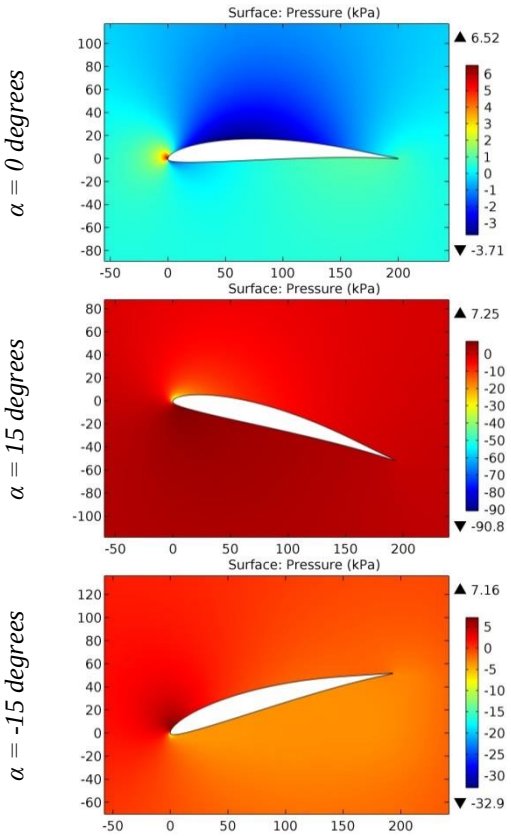

Figure 12. The pressure contours on the surfaces of the DAE-51 airfoil.

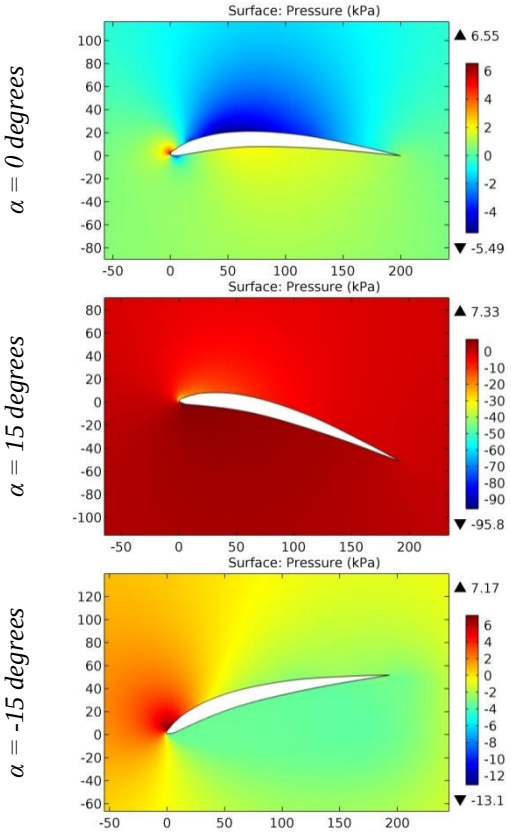

Figure 13. The pressure contours on the surfaces of the DAN-MP airfoil.

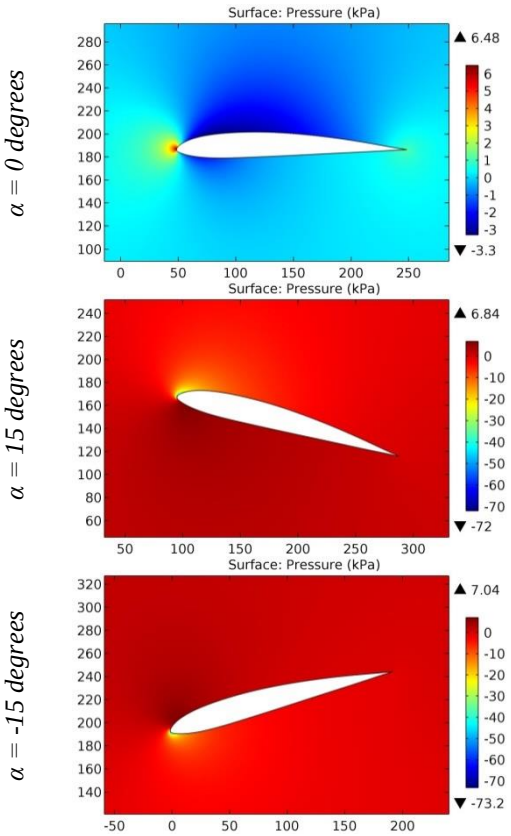

Figure 14. The pressure contours on the surfaces of the David Fraser DF 101 airfoil.

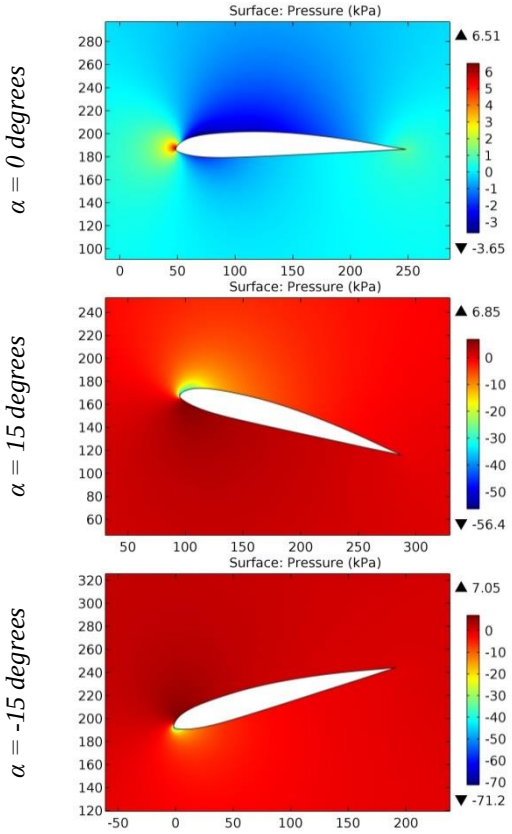

Figure 15. The pressure contours on the surfaces of the David Fraser DF 102 airfoil.

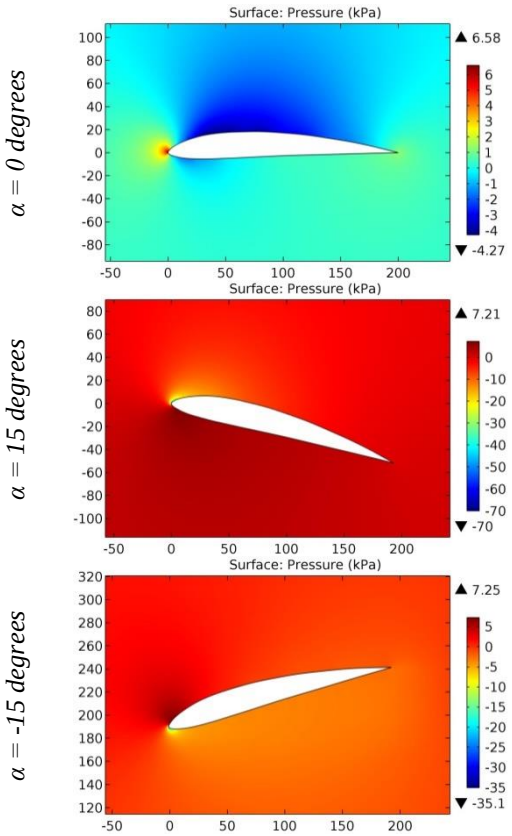

Figure 16. The pressure contours on the surfaces of the Davis airfoil.

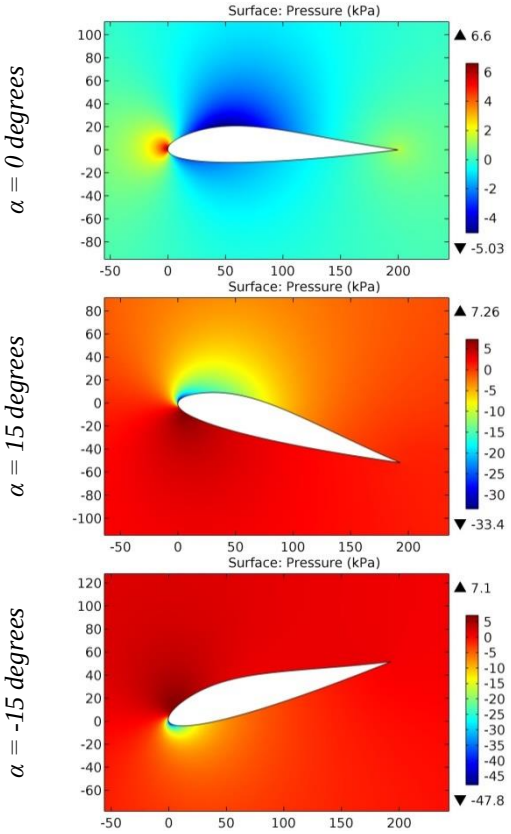

Figure 17. The pressure contours on the surfaces of the DAVIS BASIC B-24 WING airfoil.

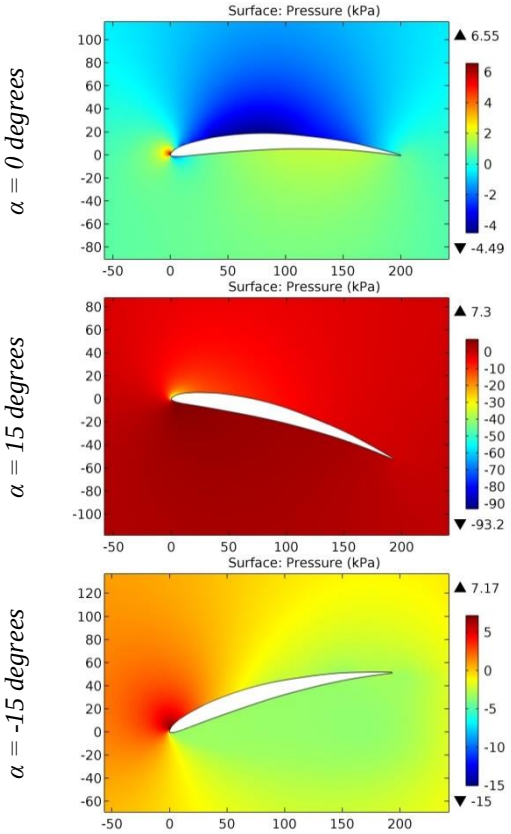

Figure 18. The pressure contours on the surfaces of the DAVIS-N airfoil.

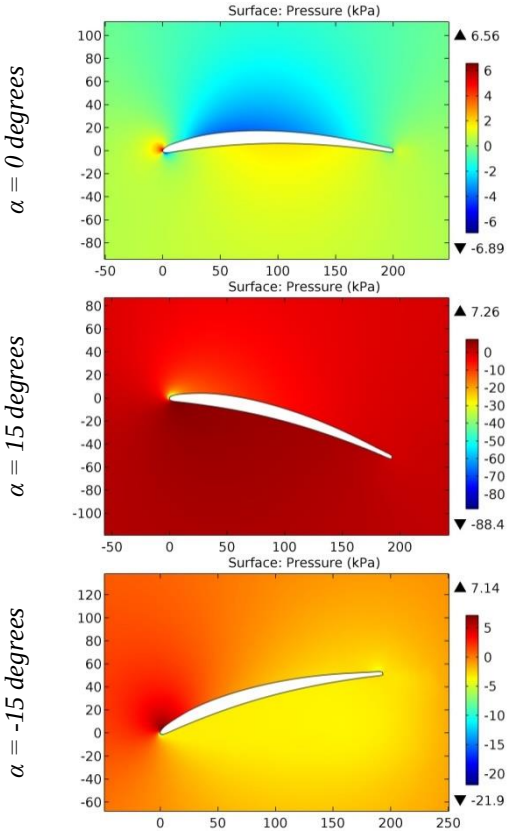

Figure 19. The pressure contours on the surfaces of the davissm airfoil.

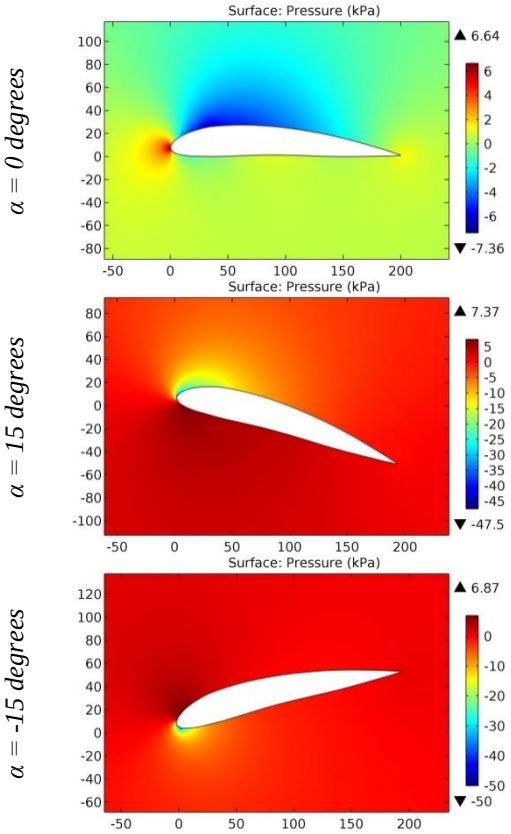

Figure 20. The pressure contours on the surfaces of the Dayton-Wright T-1 airfoil.

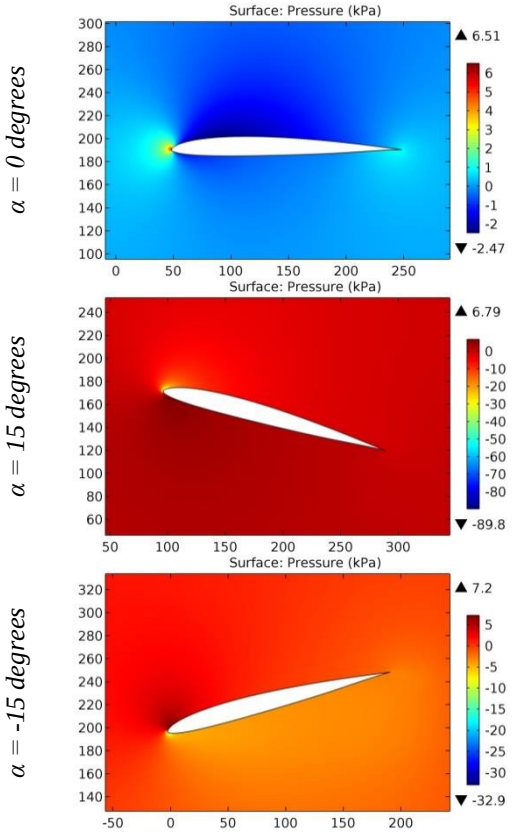

Figure 21. The pressure contours on the surfaces of the dd928416 airfoil.

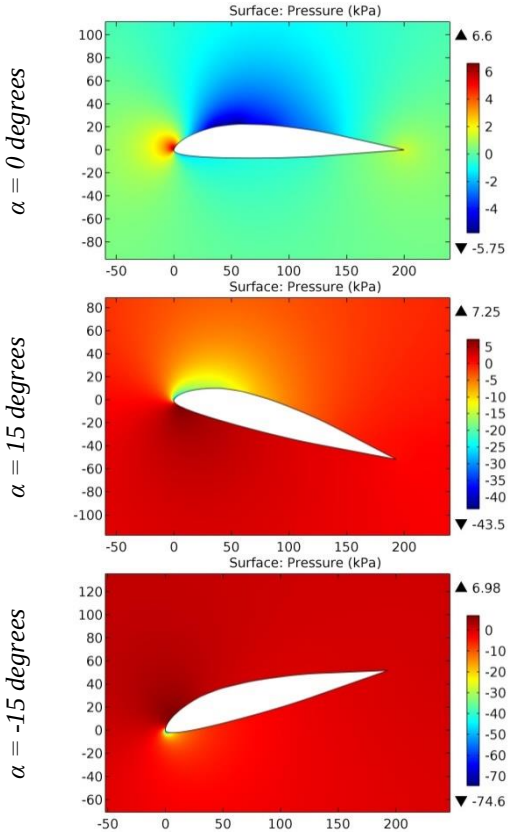

Figure 22. The pressure contours on the surfaces of the DEFIANT CANARD BL110 airfoil.

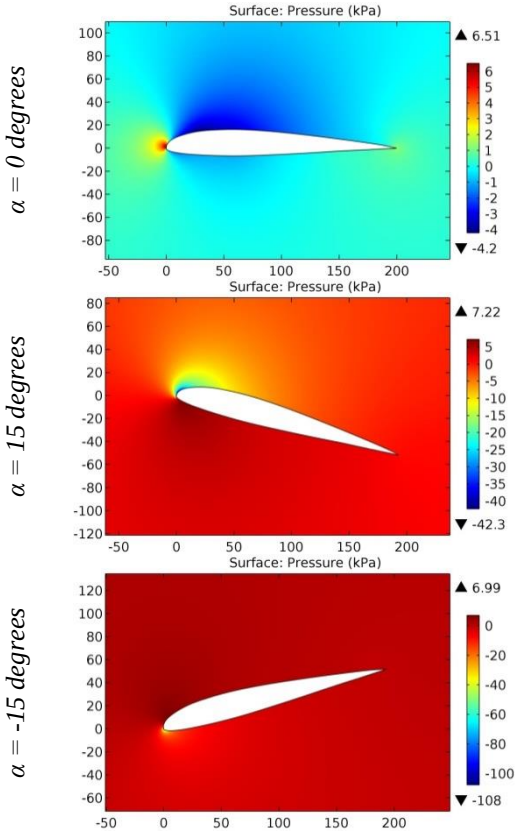

Figure 23. The pressure contours on the surfaces of the DEFIANT CANARD BL145 airfoil.

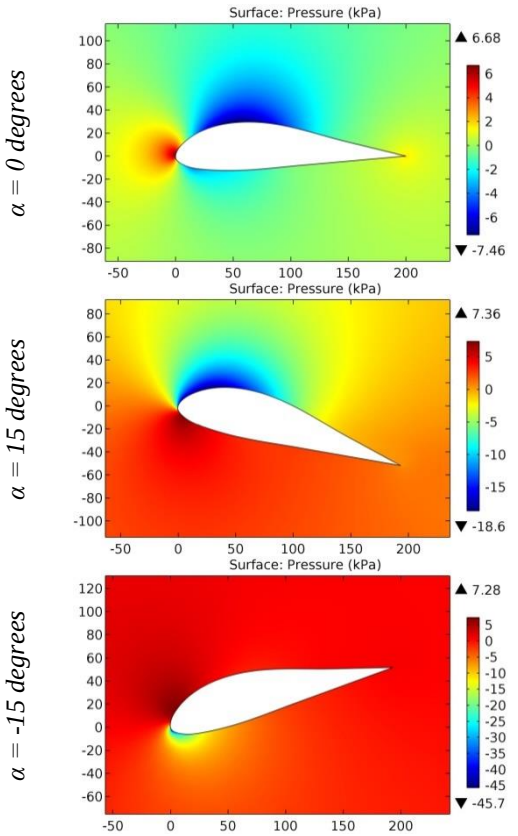

Figure 24. The pressure contours on the surfaces of the DEFIANT CANARD BL20 airfoil.

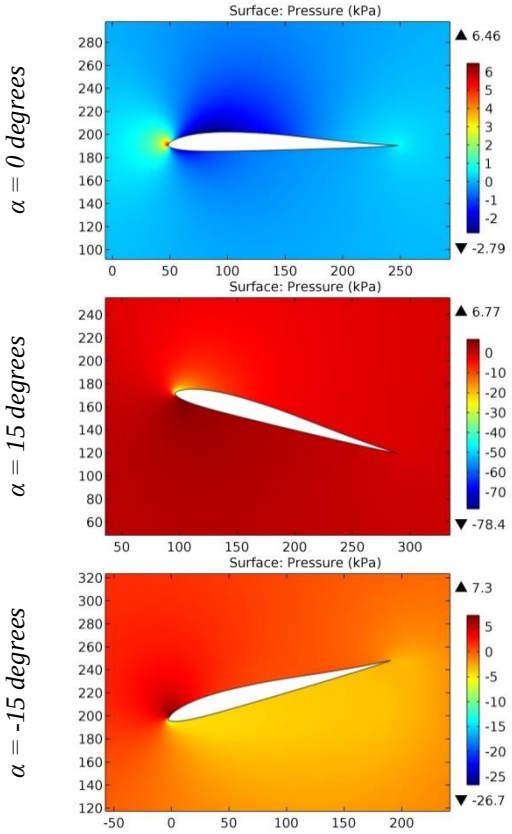

Figure 25. The pressure contours on the surfaces of the Delta 400 airfoil.

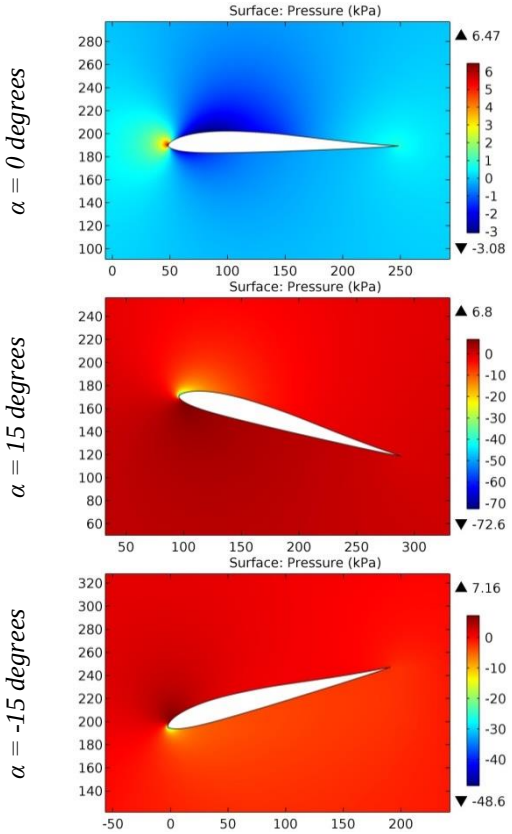

Figure 26. The pressure contours on the surfaces of the Delta 400 + 13% airfoil.

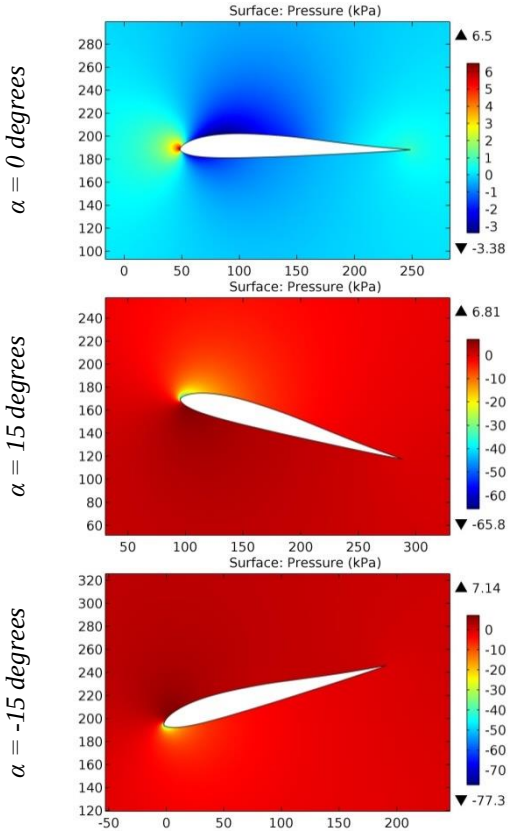

Figure 27. The pressure contours on the surfaces of the Delta 400 + 26% airfoil.

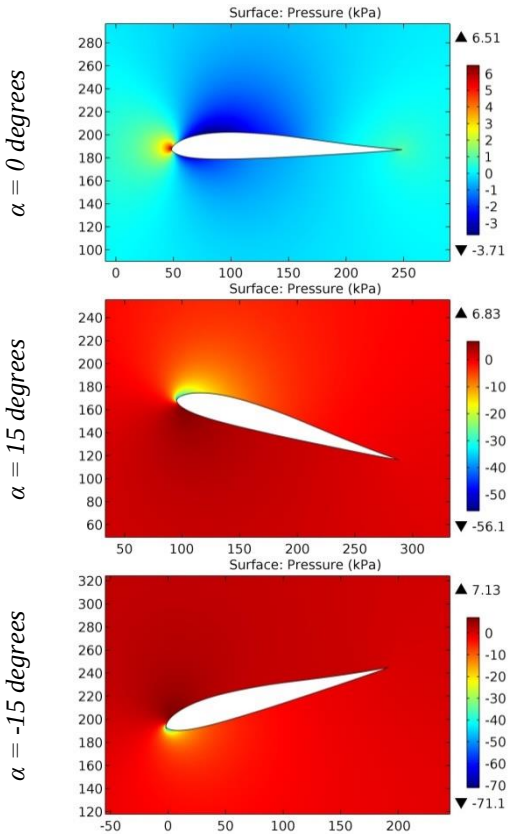

Figure 28. The pressure contours on the surfaces of the Delta 400 + 40% airfoil.

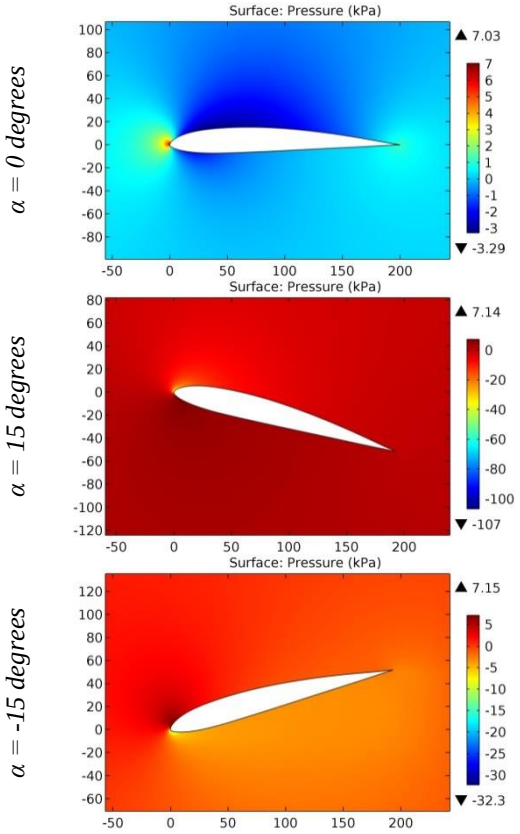

Figure 29. The pressure contours on the surfaces of the DF 101 airfoil.

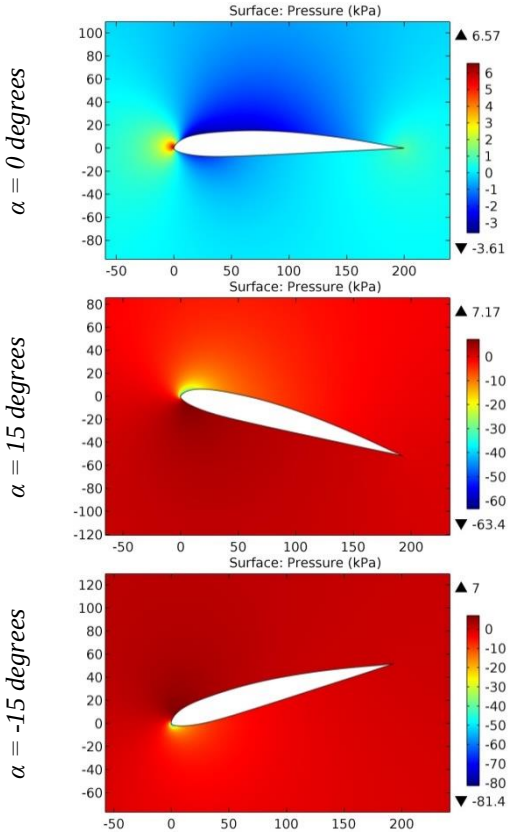

Figure 30. The pressure contours on the surfaces of the DF102 airfoil.

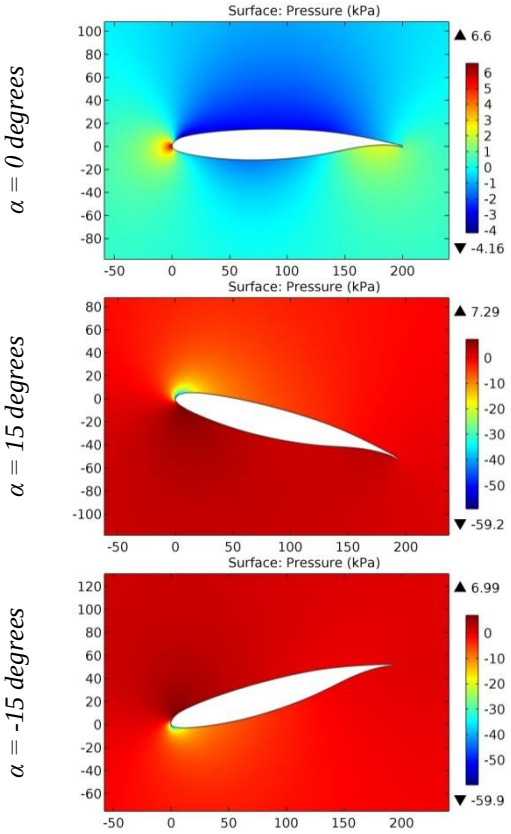

Figure 31. The pressure contours on the surfaces of the DFVLR R-4 airfoil.

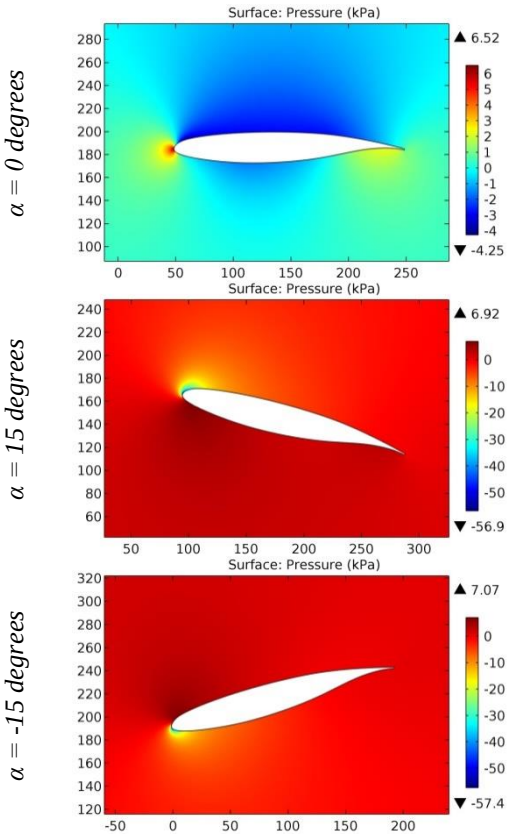

Figure 32. The pressure contours on the surfaces of the DFVLR R-4 transonic airfoil.

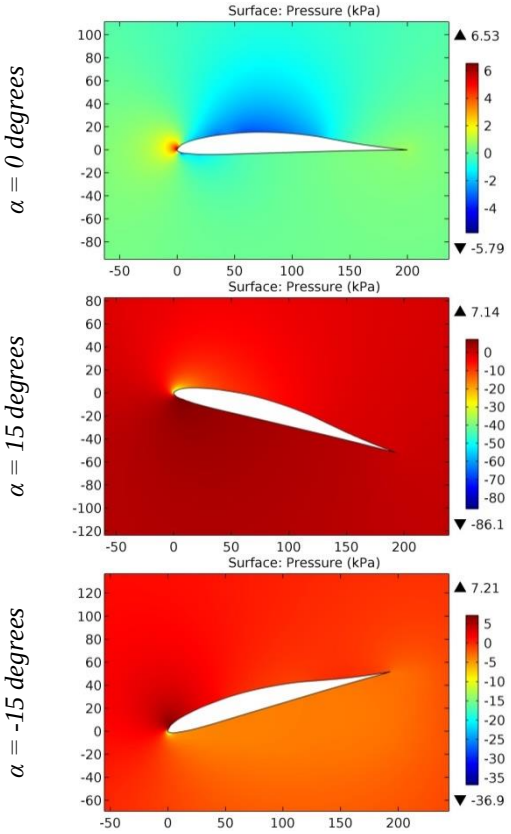

Figure 33. The pressure contours on the surfaces of the DFVLR RA 02 airfoil.

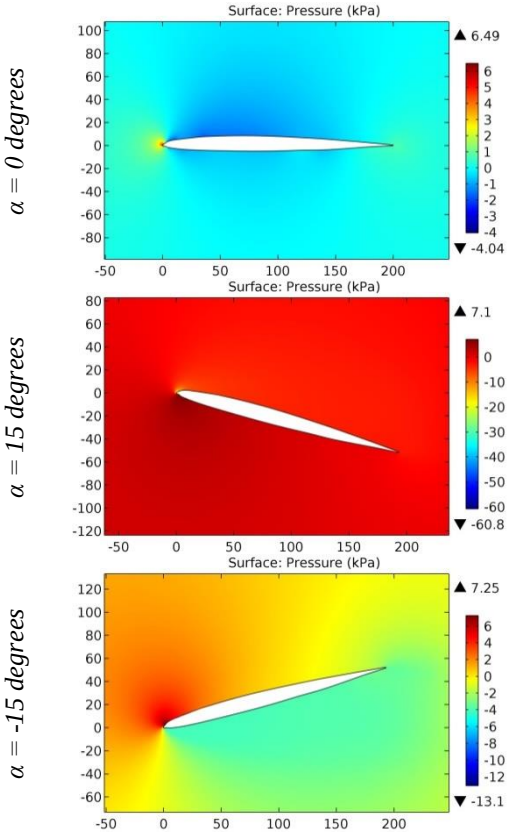

Figure 34. The pressure contours on the surfaces of the DGA 1182 airfoil.

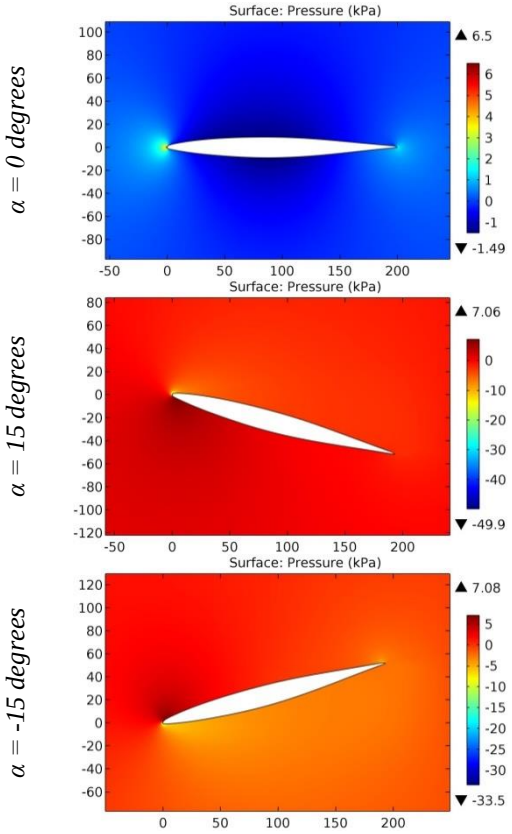

Figure 35. The pressure contours on the surfaces of the dh4009sm airfoil.

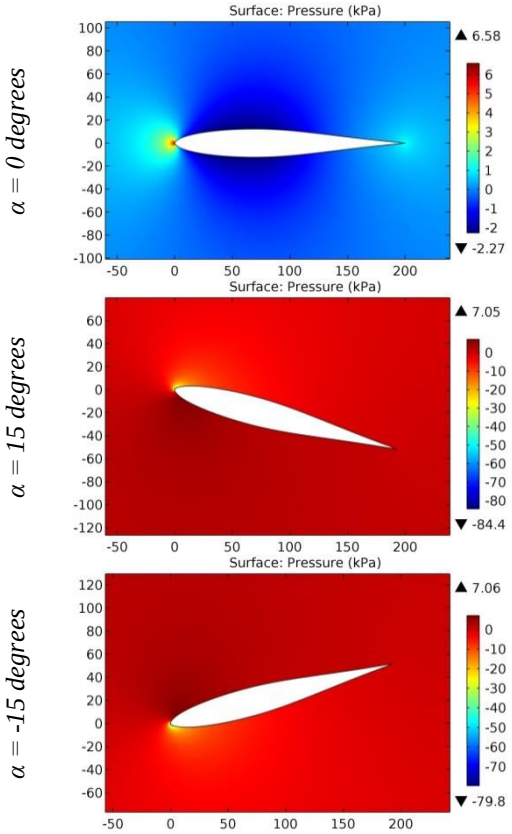

Figure 36. The pressure contours on the surfaces of the Dicke 12,28% airfoil.

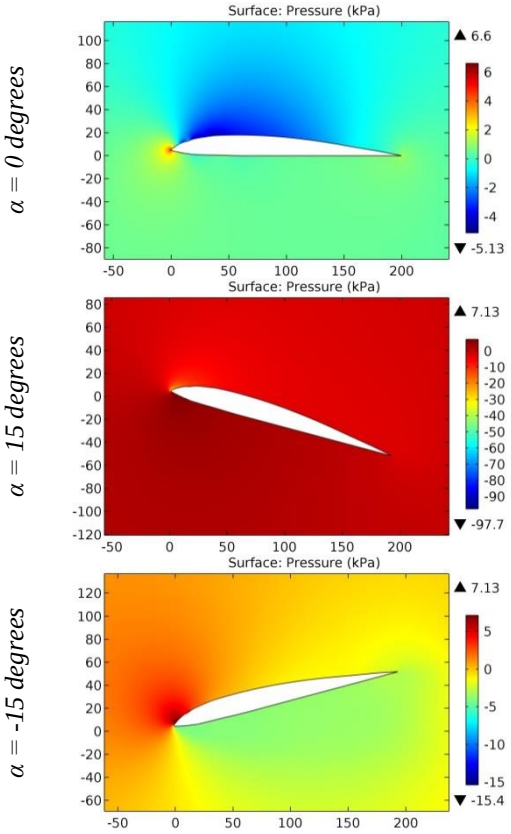

Figure 37. The pressure contours on the surfaces of the Dormoy airfoil.

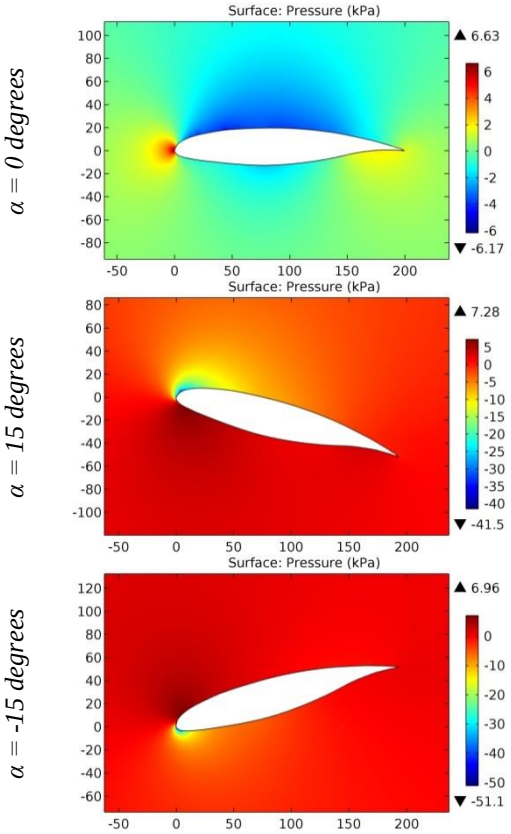

Figure 38. The pressure contours on the surfaces of the DORNIER A-5 airfoil.

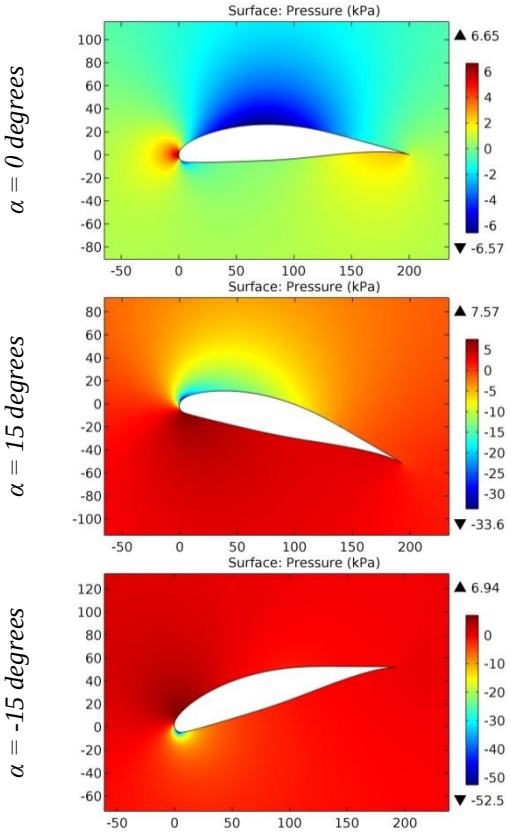

Figure 39. The pressure contours on the surfaces of the DOUGLAS LA203A airfoil.

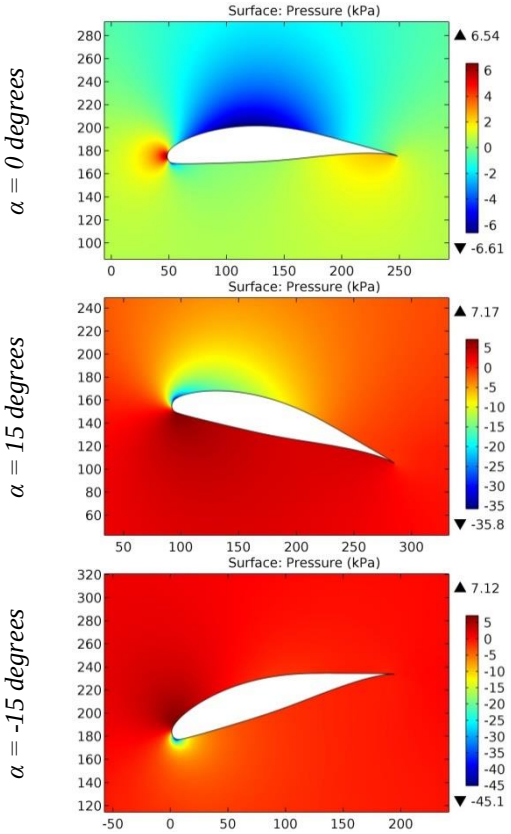

Figure 40. The pressure contours on the surfaces of the Douglas/Liebeck LA203A airfoil.

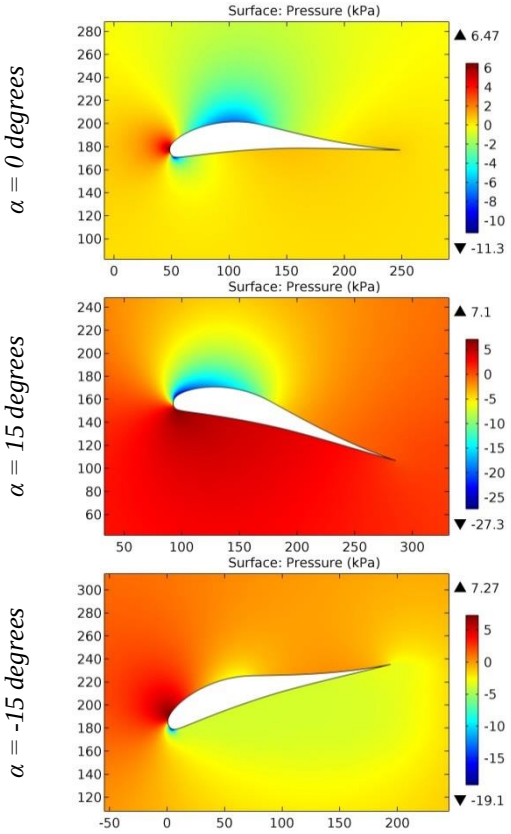

Figure 41. The pressure contours on the surfaces of the Douglas/Liebeck LNV109A airfoil.

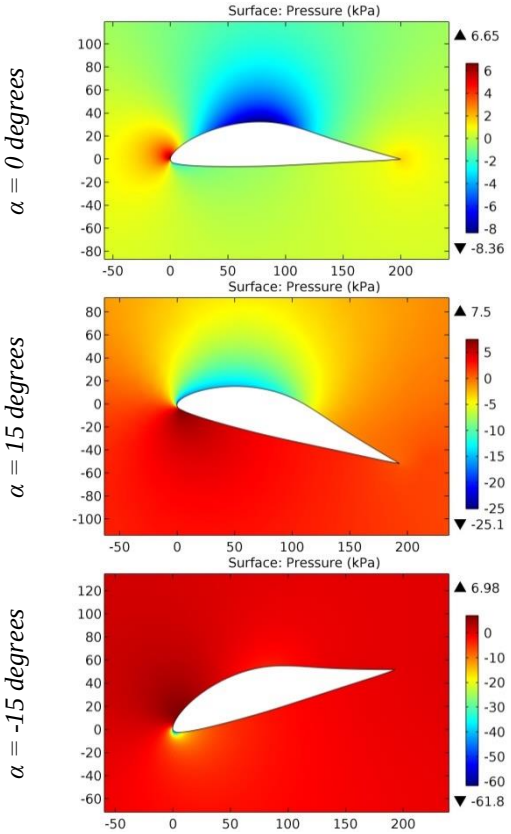

Figure 42. The pressure contours on the surfaces of the DRAGONFLY CANARD airfoil.

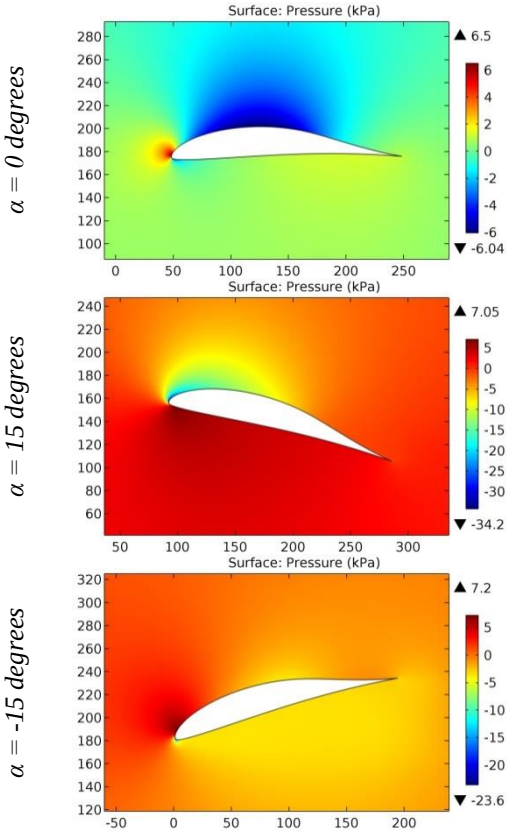

Figure 43. The pressure contours on the surfaces of the Drela DAE11 airfoil.

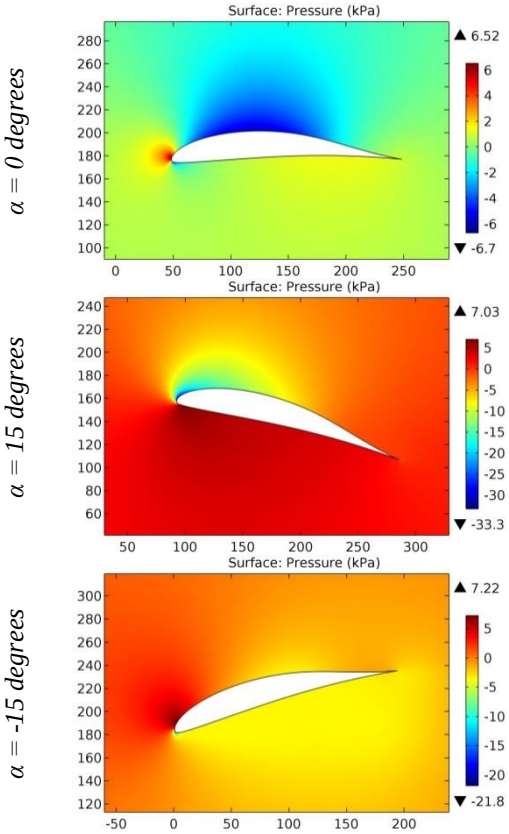

Figure 44. The pressure contours on the surfaces of the Drela DAE21 airfoil.

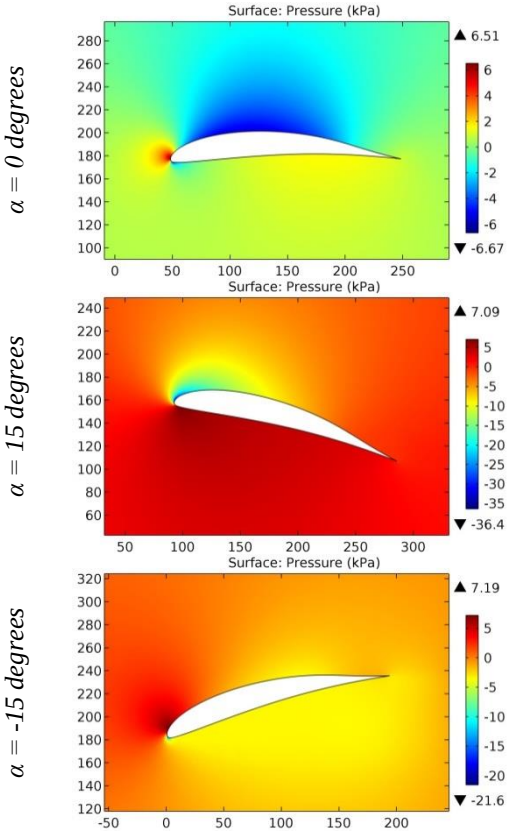

Figure 45. The pressure contours on the surfaces of the Drela DAE31 airfoil.

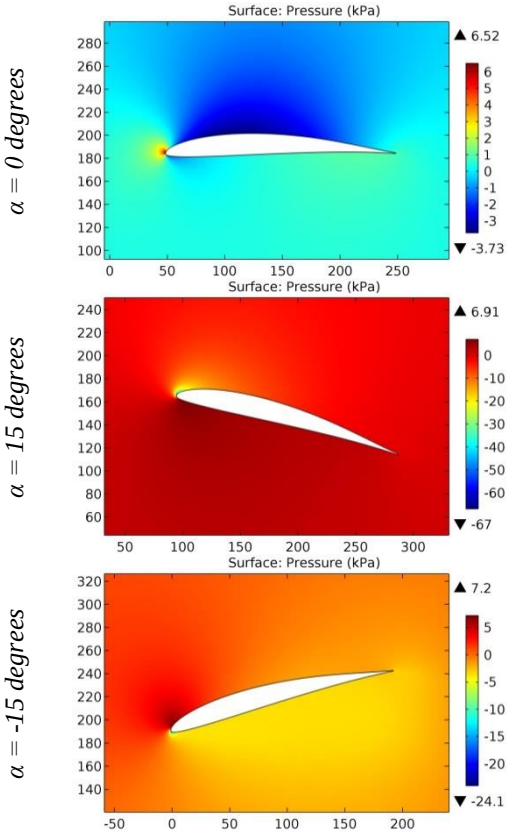

Figure 46. The pressure contours on the surfaces of the Drela DAE51 airfoil.

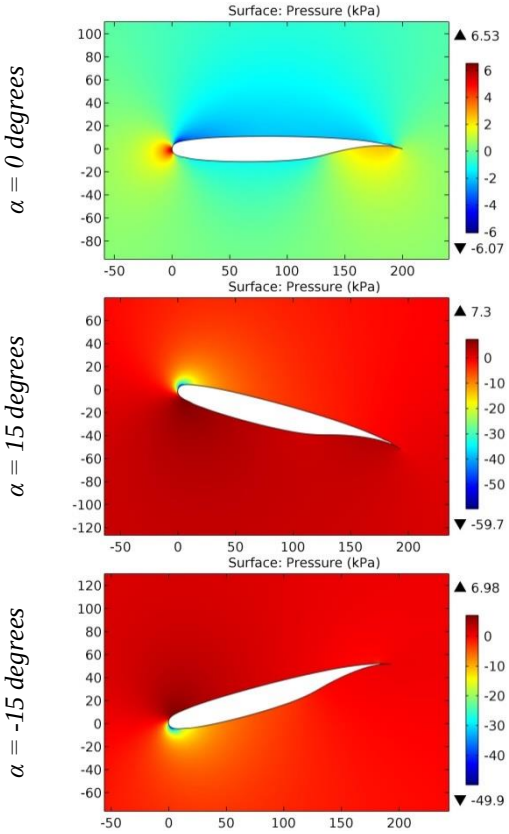

Figure 47. The pressure contours on the surfaces of the DSMA-523A airfoil.

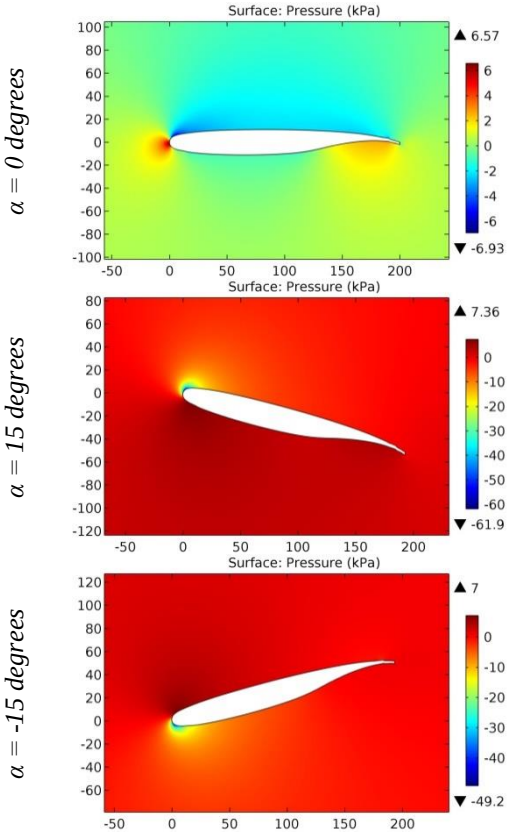

Figure 48. The pressure contours on the surfaces of the DSMA-523B airfoil.

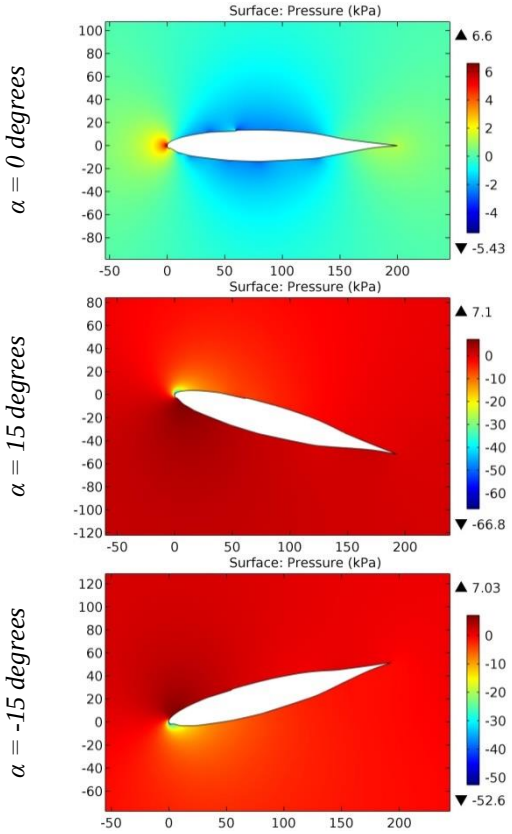

Figure 49. The pressure contours on the surfaces of the DU 86-137-25 airfoil.

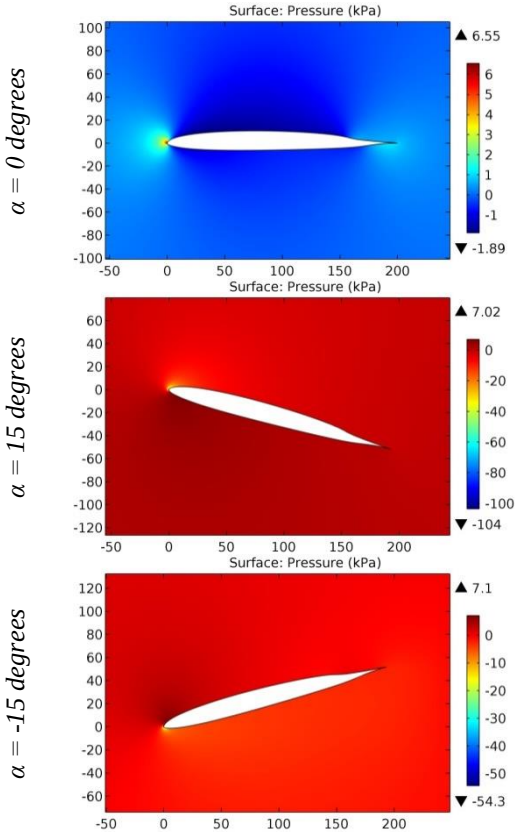

Figure 50. The pressure contours on the surfaces of the DU86-084-18 8,44% airfoil.

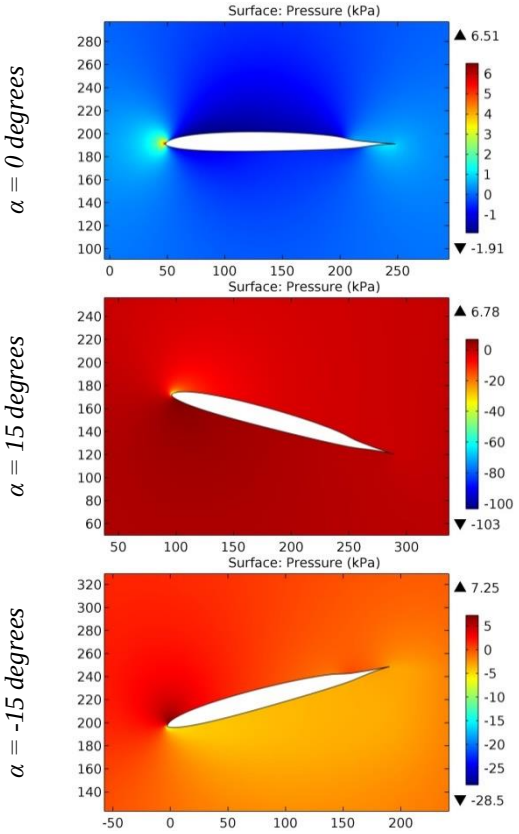

Figure 51. The pressure contours on the surfaces of the DU868418 airfoil.

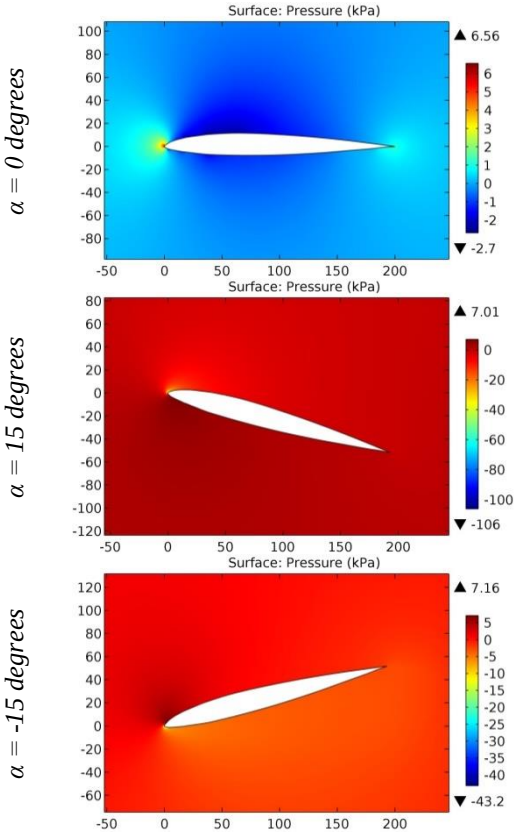

Figure 52. The pressure contours on the surfaces of the Dunham airfoil.

The maximum increase in pressure on the surfaces occurs at the angle of attack of -15 degrees for some airfoils (David Fraser DF 101, David Fraser DF 102, DAVIS BASIC B-24 WING, Dayton-Wright T-1, DEFIANT CANARD BL110, DEFIANT CANARD BL145, DEFIANT CANARD BL20, Delta 400 + 26%, Delta 400 + 40%, DF102, DFVLR R-4, DFVLR R-4 transonic airfoil, DORNIER A-5, DOUGLAS LA203A, Douglas/Liebeck LA203A, DRAGONFLY CANARD). The maximum increase in pressure on the surfaces occurs at the angle of attack of 15 degrees for the remaining airfoils.

Conclusion

The greatest drag occurs at the leading edge of the DF 101 asymmetric airfoil in conditions of horizontal flight of the airplane. This is facilitated by the less rounded leading edge. The large lift develops during the climb by the airplane having the wing with the DA0101 airfoil. However, the airplane's descent with the same airfoil leads to a reduction in the lift by more than 10 times.

References:

1. Anderson, J. D. (2010). Fundamentals of Aerodynamics. *McGraw-Hill, Fifth edition*.
2. Shevell, R. S. (1989). Fundamentals of Flight. *Prentice Hall, Second edition*.
3. Houghton, E. L., & Carpenter, P. W. (2003). Aerodynamics for Engineering Students. *Fifth edition, Elsevier*.
4. Lan, E. C. T., & Roskam, J. (2003). Airplane Aerodynamics and Performance. *DAR Corp*.
5. Sadraey, M. (2009). Aircraft Performance Analysis. *VDM Verlag Dr. Müller*.
6. Anderson, J. D. (1999). Aircraft Performance and Design. *McGraw-Hill*.
7. Roskam, J. (2007). Airplane Flight Dynamics and Automatic Flight Control, Part I. *DAR Corp*.
8. Etkin, B., & Reid, L. D. (1996). Dynamics of Flight, Stability and Control. *Third Edition, Wiley*.
9. Stevens, B. L., & Lewis, F. L. (2003). Aircraft Control and Simulation. *Second Edition, Wiley*.
10. Chemezov, D., et al. (2021). Pressure distribution on the surfaces of the NACA 0012 airfoil under conditions of changing the angle of attack. *ISJ Theoretical & Applied Science, 09 (101)*, 601-606.
11. Chemezov, D., et al. (2021). Stressed state of surfaces of the NACA 0012 airfoil at high angles of attack. *ISJ Theoretical & Applied Science, 10 (102)*, 601-604.
12. Chemezov, D., et al. (2021). Reference data of pressure distribution on the surfaces of airfoils having the names beginning with the letter A (the first part). *ISJ Theoretical & Applied Science, 10 (102)*, 943-958.
13. Chemezov, D., et al. (2021). Reference data of pressure distribution on the surfaces of airfoils having the names beginning with the letter A (the second part). *ISJ Theoretical & Applied Science, 11 (103)*, 656-675.
14. Chemezov, D., et al. (2021). Reference data of pressure distribution on the surfaces of airfoils having the names beginning with the letter B. *ISJ Theoretical & Applied Science, 11 (103)*, 1001-1076.